



## A strategy to reconstruct the broad features of the acoustic impedance profile from band-limited seismic reflection data

Animesh Mandal<sup>1\*</sup>, and S. K. Ghosh<sup>2</sup>, <sup>1</sup>Department of Earth Sciences, IIT Kanpur, India; <sup>2</sup>Theoretical Modeling Group, CSIR-National Geophysical Research Institute, Hyderabad, India

Email: [animeshm@iitk.ac.in](mailto:animeshm@iitk.ac.in)

### Keywords

Reflection data, Acoustic impedance, Broadband, Singular Value Decomposition, Inversion

### Summary

Estimation of acoustic impedance from reflection data is an essential step for quantitative interpretation of seismic data. However, the band limitation of reflection seismic data (in particular the absence of low frequencies) hinders a direct interpretation in terms of rock properties owing to nonuniqueness of the solution. The existing methods counter the nonuniqueness either by stabilizing the answer with respect to an initial model or by resorting to an assumption of certain criterion such as sparsity of the reflection coefficients. Using a layered earth model and the basic amplitude equation we formulate a set of linear equations where the recursively integrated reflection trace amplitudes constitute the data and reflection coefficients are the unknowns. The local layercake assumption and the strategy of seeking singular value decomposition (SVD) solution of the formulated linear equations counter the nonuniqueness by aiming only for the low frequency part of the impedance profile. The efficacy of the proposed approach has been tested with synthetic data containing significant noise for a simple earth model as well as the real earth represented by well log impedance data. Additional advantages of the method include accurate estimates of the impedance mean, and approximate reconstruction of the trend of the impedance profile. All of these can serve as important constraints for an effective earth modeling.

### Introduction

Seismic derived acoustic impedance is the final as well as essential output for quantitative interpretation of seismic data. It is the only natural bridge between the well logs and the observed seismic data (Lindseth, 1979) and therefore, basic to extract the detailed subsurface lithology. However, the band limitation of observed seismic reflection data leads to imperfect calculation of the acoustic impedance, i.e., the subsurface geology. According to Ghosh (2000) the impulse response for reflection,  $R(t)$  is proportional to the derivative (w. r. to time) of the logarithm of acoustic impedance,  $t$  denoting the two-way travel time. Thus, for an imperfect, i.e., band-limited version of  $R(t)$ , the resulting reconstruction of the impedance function would also be imperfect and nonunique. A reasonable estimate of the

impedance profile would, however, require a broadband estimate of  $R(t)$  and would need to overcome the nonuniqueness employing either auxiliary information, often nonseismic or constraints characterizing the impedance model. Historically the issue of nonuniqueness has been addressed in a variety of ways, e.g., with an initial model or by resorting to an assumption of certain criterion such as sparsity of the reflection coefficients etc. (Yilmaz, 2000). Therefore, the reconstruction of acoustic impedance from the band-limited seismic reflection data remains to be one of the greatest challenges to the geoscientists dealing with seismic exploration study.

In this paper we have proposed a new method based on the nominal assumption of an earth model consisting of a stack of homogeneous and horizontal layers, and derives the emerging reflection coefficients employing only the basic physics of reflection seismic as rooted in Ghosh (2000). In order to implement the method the reflection data must be processed in the following manner. First, an estimated embedded wavelet has to be deconvolved from the seismic trace in a band where the wavelet has significant amplitude. The resulting trace is recursively integrated to yield the normalized logarithmic impedance (NLI) data. The integration can effectively be accomplished by a convolution between the deconvolved trace and the band-limited Heaviside function (Ghosh, 2000). Next, a set of linear equations is formulated which is solved for the unknown reflection coefficients, arising from the assumed layered earth and employing the NLI data. Three bands are employed in order to arrive at consistent estimates of broad features of the impedance profile. Nyquist criterion constrains the number of non-redundant sample points. Nonuniqueness is overcome partly by limiting the number of layers to the number of sample points and partly by resorting to singular value decomposition (SVD) method of solving the set of linear equations. The efficacy of the proposed method has been demonstrated with synthetic data with and without noise generated from a rudimentary model and from a measured log of acoustic impedance.

### Mathematical formulation: part I

According to Ghosh (2000)  $A_b$ , the reconstructed impedance function for a vertically inhomogeneous layered

## Low frequency impedance reconstruction

earth model with upper and lower band limits of data as  $f_H$  and  $f_L$ , is given by

$$\ln \left[ \frac{A_b(t)}{A_0} \right] = 2R(t) * \left( \frac{1}{\pi} \right) (\text{Si } 2\pi f_H t - \text{Si } 2\pi f_L t), \quad (1)$$

where the left hand side (LHS) is designated as NLI,  $\text{Si } x = \int_0^x \left( \frac{\sin u}{u} \right) du$ ,  $*$  denotes convolution, and  $A_0$  is the impedance at some reference time  $t_0$ , typically, the time reckoned as zero. The second term in the convolution above is the band-limited Heaviside function, denoted by  $H_b(t)$ . In this approach, we have assumed  $n$  reflection coefficients occurring in the window of reflection time under consideration. Let a typical reflection coefficient  $r_k$  occurs at  $t=t_k$ . Then the impulse response  $R(t)$  can be written as

$$R(t) = \sum_{k=1}^n r_k \delta(t - t_k). \quad (2)$$

Thus, the equation (1) can be rewritten as

$$\ln \left[ \frac{A_b(t)}{A_0} \right] = 2 \sum_{k=1}^n r_k H_b(t - t_k). \quad (3)$$

When the equation (3) is recast in sampled form, then both the  $H_b(t-t_k)$  and the LHS, designated as  $a(t)$ , have to be sampled adequately and the equation can be rewritten as

$$\mathbf{G}\mathbf{r} = \mathbf{a}, \quad (4)$$

where  $\mathbf{G}$  is a matrix whose  $k^{\text{th}}$  column consists of the sampled values of  $H_b(t - t_k)$ ,  $\mathbf{r}$  is a column vector  $[r_1, r_2, \dots, r_n]^T$  corresponding respectively to times  $t_1, t_2, \dots, t_n$ , and  $\mathbf{a}$  is a column vector consisting of the sampled values of  $a(t)$ , i.e., NLI, restricted to a given time range. As  $H_b(t)$  is both anticausal and antisymmetric but practically time limited (Ghosh, 2000). Thus, we consider all vectors  $H_b(t-t_k)$  and their weighted sum  $\mathbf{a}$  in the time range  $(t_1 - t_A) \leq t \leq (t_n + t_A)$ , where  $t_1$  and  $t_n$  are respectively the reflection times corresponding to the first and the last reflectors, and  $t_A$  is the additional time span attached both before  $t_1$  and after  $t_n$ , arising from the effective span of  $H_b(t)$  (Figure 1). With the range of  $t$  fixed thus,  $(t - t_k)$  will range according to  $(t_1 - t_A - t_k) \leq (t - t_k) \leq (t_n + t_A - t_k)$ . For given  $f_L, f_H$  and a uniform time-step between all successive  $t_k$  and  $t_{k+1}$ , the matrix  $\mathbf{G}$  is fully known. Now, if  $\mathbf{r}$  is known then we can solve the forward problem and generate the NLI data. For forward problem time-steps are the actual known reflector locations. On the other hand for inverse problem to determine the column vector  $\mathbf{r}$  we use the known value of  $\mathbf{a}$  and  $\mathbf{G}$ , where the matrix  $\mathbf{G}$  is constructed from the time-step equaling the Nyquist sampling interval corresponding to  $f_H$ . Thus, for forward problem, the number of columns in  $\mathbf{G}$  is same as the number of reflectors in the actual model but in inverse problem number of columns of  $\mathbf{G}$  is same as the number of uniformly spaced reflectors hypothesized for the respective frequency bands on the basis of Nyquist criterion. Thus, the equation (4) can now be solved for the unknown reflection coefficients by the method of least squares provided  $\mathbf{a}$ , is derived from either field data (as mentioned in the 'introduction' section) or synthetic data.

### Tests on a simple model

The synthetic normalized logarithmic impedance (NLI) data has been generated using equation (4) and assuming a constant density value, velocity value,  $t_A = 150$  ms,  $f_L = 10$  Hz and  $f_H = 100$  Hz. The  $r_k, t_k$ , and the velocity at time  $t = 0$  for the model is listed in Table 1. We assume equispaced  $t_k$ 's in the time span of interest to solve for the reflection coefficients, i.e., for inversion. The time-step between successive  $t_k$ , was chosen as 5 ms, corresponding to the Nyquist rate for  $f_H = 100$  Hz. Once the reflection coefficients are known, the velocity profile is reconstructed from the known initial velocity and presented as an overplot on the initial velocity profile (Figure 2a, upper panel). It is evident that there is practically no error in reconstruction. The NLI data used for reconstruction and the hypothetical NLI data that the reconstructed models would give rise to also match remarkably well (Figure 2a; lower panel). Another remarkable outcome is that though the reflectors are postulated at every  $t_k$ , the nonreflected reflection coefficients corresponding to the nonreflecting horizons in the original model turn out to be zero.

Next, a noise (a random series of reflection coefficients occurring according to a white Gaussian distribution) has been added to the synthetic data in order to test the tolerance of the algorithm to error, arising from either data gathering or model specification. The S/N ratio is kept at about 10% (Figure 2b). Here the S/N ratio refers to the ratio of the energy of the NLI data and that of the error added to it. The overplot of the reconstructed velocity over the original, and the noisy NLI data (used for reconstruction) over the hypothetical NLI data (that the reconstructed models would give rise) has been displayed in upper panel and lower panel, respectively of Figure 2c. The r.m.s. misfit in this case is 0.007. Thus, on the whole the reconstruction is excellent.

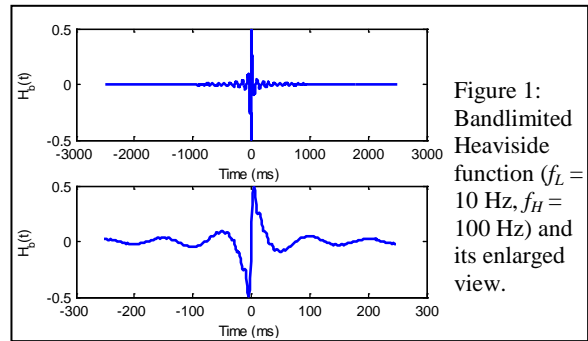
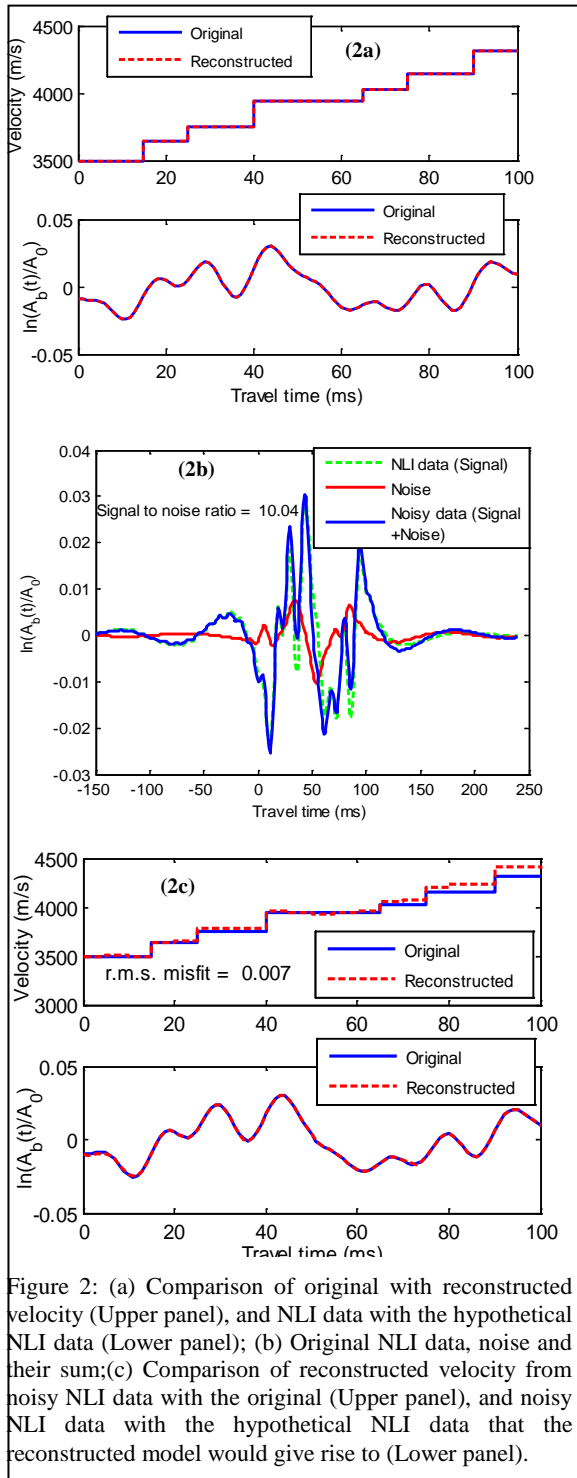


Figure 1: Bandlimited Heaviside function ( $f_L = 10$  Hz,  $f_H = 100$  Hz) and its enlarged view.

$r_k$ values	$t_k$ values (ms)	Velocity at $t=0$ (m/s)
0.02, 0.015, 0.025, 0.01, 0.015, 0.02	15, 25, 40, 65, 75, 90	3500

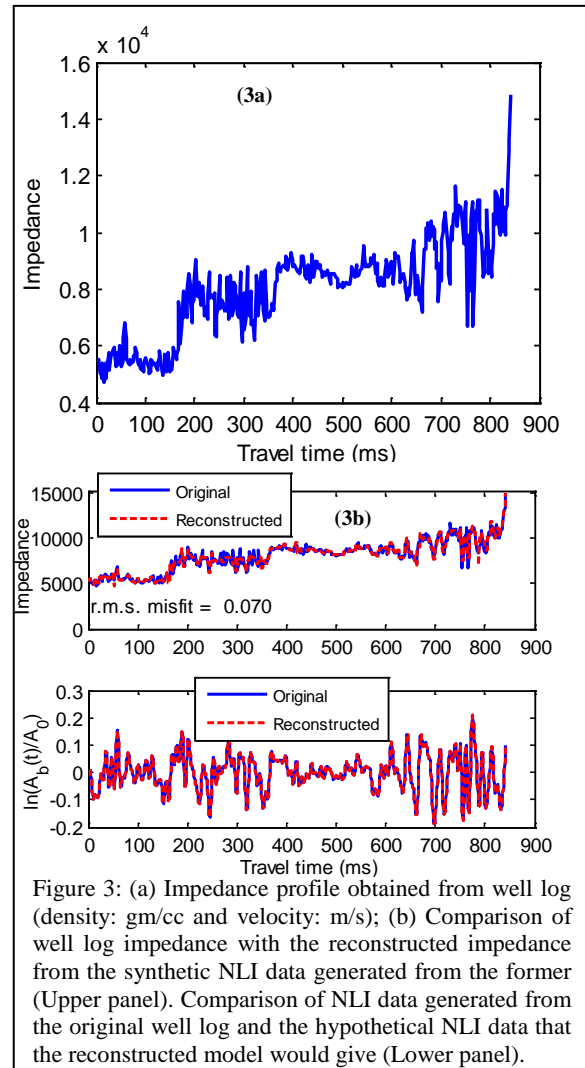
Table 1: Reflection coefficients ( $r_k$ ), time ( $t_k$ ), and velocity at  $t = 0$ , for simple layered earth model.

## Low frequency impedance reconstruction



### Test on impedance model obtained from well log

Figure 3a depicts an impedance profile obtained from well log sampled at every 2 ms. The synthetic NLI data has been generated from it and then employ the same NLI data to recover the reflection coefficients and the resulting impedance profile. In absence of noise, for  $f_L = 8\text{Hz}$ ,  $f_H = 100\text{Hz}$  and the time-step = 2 ms, it was possible to reconstruct the acoustic impedance profile remarkably well (Figure 3b). However, in the presence of even the slightest of noise, the above procedure yields rather absurd and unstable results. The reasons for the failure to handle noise can be traced to the extremely small singular values of the matrix  $G$ , employed in the least squares solution (Press et al., 1992). The remedy for instability lies in discarding the small singular values and obtaining a solution, as discussed in the next section.



## Low frequency impedance reconstruction

### Mathematical formulation: part II

#### Singular Value Decomposition (SVD)

According to SVD theorem any  $m \times n$  matrix  $G$  whose number of rows  $m$  is greater than or equal to its number of columns  $n$ , can be decomposed as

$$G = U\Sigma V^T, \quad (5)$$

where  $U$  is a  $m \times n$  column-orthogonal matrix,  $\Sigma$  is a  $n \times n$  diagonal matrix with diagonal entries  $\sigma_1, \sigma_2, \sigma_3, \dots, \sigma_n$ , all nonnegative and ordered according to  $\sigma_1 > \sigma_2 > \sigma_3 > \dots > \sigma_n$ ; and  $V$  is an  $n \times n$  orthogonal matrix. The diagonal elements of  $\Sigma$  are called the singular values of  $G$ . The formal least squares solution of the system  $Gr = \mathbf{a}$  (Eq. 4) turns out to be

$$\mathbf{r} = V\Sigma^{-1}U^T\mathbf{a}, \quad (6)$$

where  $\Sigma^{-1}$  is a  $n \times n$  diagonal matrix with diagonal elements  $\sigma_1^{-1}, \sigma_2^{-1}, \sigma_3^{-1}, \dots, \sigma_n^{-1}$ . Thus, it is obvious that the existence of very small singular values would tend to amplify the error of computation and that in data  $\mathbf{a}$ , while implementing the last equation. In such cases, instead of discarding a smaller singular value and zeroing its reciprocal, another option is to artificially enhance the magnitude of a singular value appreciably such that its reciprocal no longer blows up. This will lead to a smoother solution with smaller least squares residuals (Press et al., 1992; Indira and Gupta, 1998) and thus, help to obtain the broad trend of the impedance profile.

In order to obtain the best possible solution for the impedance profile, we truncate the singular value series at a certain small singular value ( $\sim 10^{-2}$ ), designated as the terminal singular value and construct three following sets.

- (a) We retain the set of singular values unmodified.
- (b) We replace the current terminal value with its harmonic mean with the next higher singular value, while the rest of the set remains unchanged.
- (c) We replace the current terminal value with the next higher singular value, while the rest of the set remains unchanged.

The above three choices would give rise to three categories for a group characterized by an unmodified terminal singular value (UTSV) and two modified ones. In moving across the choices from (a) to (b) and then to (c) the effective terminal singular value successively increases. This should result in progressively smoother reconstruction of the impedance profile. The truncation of the set of singular values and computation of the impedance profiles resulting from the above choices can be repeated gradually and systematically. Eventually a stage should come when the impedance profiles would be practically insensitive to the excursion across the choices (a) through (c). At this stage the solution for the impedance profile can be said to have reached a saturation stage, i.e., solution become oversmooth. However, a less smooth solution would be

more realistic and desirable. Accordingly, we would come back one step to the case when the next smaller singular value was the unmodified terminal singular value (UTSV).

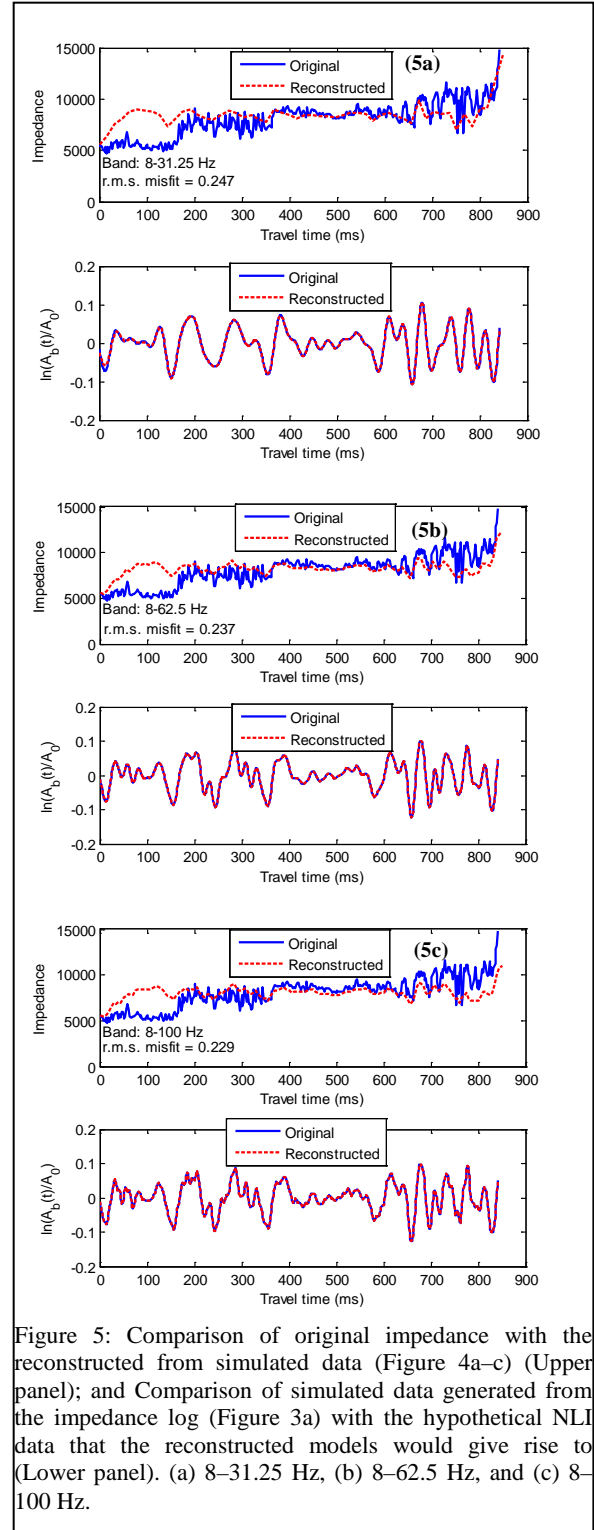
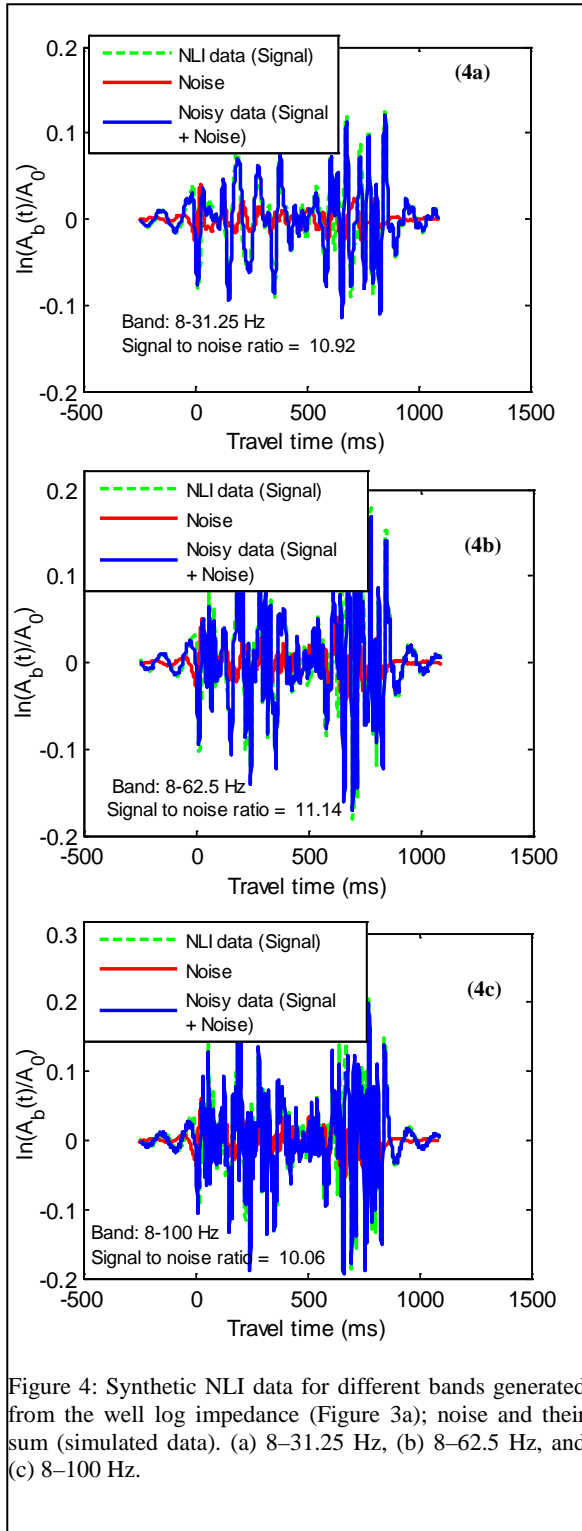
#### Simulating noisy data

Synthetic NLI data is computed employing equation (4) for the choice  $t_A = 250$  ms and the impedance profile acquired from the well log displayed in Figure 3a for three bands, namely, 8–31.25 Hz, 8–62.5 Hz, and 8–100 Hz. In order to mimic real NLI data as would be obtained from processed reflection data; here also we add  $\sim 10\%$  noise to the synthetic data (Figure 4a–c). As we aim to reconstruct only a smoothed version of the actual impedance log, we smooth the simulated data (9 point smoothing for 8–31.25 Hz band, and other bands with 15 point smoothing). Now the reflection coefficients are estimated from the smoothed data by solving the set of linear equations encapsulated in equation (4) by way of implementing equation (6). This is carried out according to the strategy of discarding small singular values as mentioned above. Next, one obtains from the derived reflection coefficients an estimate of the impedance profile using the known value of the impedance at the initial time.

To demonstrate the efficacy of reconstruction, an overplot of the reconstructed impedance profile over the original is displayed for the three bands in Figure 5a–c (upper panels). Broad highs and lows of the actual log are well recovered in reconstruction across three bands. In addition, the simulated data used for reconstruction and the hypothetical NLI data that the reconstructed models would give rise to match remarkably well (Figure 5a–c; lower panel). The r.m.s. misfits for these reconstructions are 0.247, 0.237, and 0.229 respectively, for the above three bands. Thus, the reconstructions are also good. Here, we look for a consistent estimate of impedance across various bands. Inspection over three bands yield the following near-consistent estimates of the mean of the impedance profile: 8476 (8–31.25 Hz), 8262 (8–62.5 Hz), and 8043 (8–100 Hz) (Table 2). It is significant that these estimates and their mean of 8260 compare favorably with the actual impedance mean of 8013 of the log data. The observed consistency is persuasive enough to recommend adoption of the above approach. Once, a consistent estimate of the impedance mean is in place, estimating impedance mean for a new frequency band becomes easy.

The impedance profiles corresponding to the respective mean estimates can be treated as the reconstructed impedance profiles for the respective bands (Figure 5a–c). Alternatively, if the impedance mean can be estimated from measurements in a nearby well, then that reconstruction of the impedance profile which leads to a similar mean should be adopted as the best-estimate.

## Low frequency impedance reconstruction



## Low frequency impedance reconstruction

Table 2: Results of impedance reconstruction employing synthetic data generated from impedance log with noise for different frequency bands. Three choices of the terminal singular value in a group;  $\sigma_U = \sigma_k$  (no modification);  $\sigma_k = \sigma_H = [2\sigma_k\sigma_{k-1}/(\sigma_k + \sigma_{k-1})]$ ; and  $\sigma_k = \sigma_R = \sigma_{k-1}$ .

Frequency Band (Hz)	Time-step of $t_k$ (ms)	S/N ratio	Singular values ( $\sigma$ )		Mean of Reconstructed Impedance
			Unmodified terminal singular value (UTSV) ( $\sigma_k$ )	Actual terminal singular value	
8–31.25	16	10.92	0.15914	$\sigma_U = 0.15914$	13170
				$\sigma_H = 0.24017$	10532
				$\sigma_R = 0.48932$	8476
8–62.5	8	11.14	0.06291	$\sigma_U = 0.06291$	9939
				$\sigma_H = 0.09779$	9056
				$\sigma_R = 0.21949$	8262
8–100	5	10.06	0.07475	$\sigma_U = 0.07475$	8554
				$\sigma_H = 0.11618$	8043
				$\sigma_R = 0.26068$	7566

### Discussion

The above results successfully demonstrate possibility of a broadband reconstruction of impedance from band-limited reflection data. Therefore, our approach shows a way of solution to the problem of low frequency impedance reconstruction in seismic interpretation. Another important aspect of our scheme is that it does not have to begin with an initial model like, generalized linear inversion schemes (Cook and Schneider, 1983) and constrained sparse-spike inversion (Torres-Verdin et al., 1999). Again, the original sparse-spike inversion (SSI) scheme (Levy and Fullagar, 1981) and autoregressive modeling method of Walker and Ulrych (1983) both required the impedance structure to contain a minimum number of reflectors, however, our algorithm can have as many reflectors as the number of sample points, constrained only by the Nyquist criterion. Oldenburg et al. (1983) point out lack of uniqueness in the presence of noise, while using SSI. In comparison the proposed method is, demonstrably, noise-tolerant to a significant degree. Nonuniqueness is countered in part by modeling the earth as a stack of homogeneous and horizontal layers, and in part by the SVD method of solution. The main clue to this reconstruction lies in conceiving the model as a stack of homogeneous layers. This requires sharp boundaries and thus imposes more low and high frequencies into the solution. The SVD method used here, rejects the smaller singular values, seeks a smooth solution, and recovers the cumulative reflection coefficients over sufficiently long time span compromising the accuracy in the initial part of the impedance profile.

The method can also adapt well to a situation when the reflection coefficient at a certain interface is known. However, the real seismic data display only the relative amplitude. In order to restore the absolute amplitude one needs to determine the scale factor for restoration. The latter can be determined by calibrating the apparent reflection coefficient at certain prominent reflector against its known value availed from non-seismic information.

### Conclusions

The present work makes a case for a fresh approach for broadband impedance reconstruction by demonstrating its success on synthetic data. The major benefits of this low frequency impedance reconstruction are accurate estimate of impedance mean, and approximate estimation of impedance profile and its broad trend. These information can serve as an input for more refine inversion modeling. However, the approach may need some basic refinement for routine use in real seismic data sets.

### References

- Cooke, D. A. and Schneider, W. A., 1983, Generalized inversion of reflection seismic data; *Geophysics*, 48,665–676.
- Ghosh, S. K., 2000, Limitations on impedance inversion of band-limited reflection data; *Geophysics*, 65(3), 951–957.
- Indira, N. K. and Gupta, P. K., 1998, *Inverse Methods: General principles and application to Earth system sciences*; Narosa Publishing House, New Delhi.
- Levy, S. and Fullagar, P. K., 1981, Reconstruction of a sparse spike train from a portion of its spectrum and application to high-resolution deconvolution; *Geophysics*, 46, 1235–1243.
- Lindseth, R. O., 1979, Synthetic sonic logs – a process for stratigraphic interpretation; *Geophysics*, 44(1), 3–26.
- Oldenburg, D. W., Scheuer, T. and Levy, S., 1983, Recovery of the acoustic impedance from reflection seismograms; *Geophysics*, 48, 1318–1337.
- Press, W. H., Flannery, B. P., Teukolsky, S. A. and Vetterling, W. T., 1992, *Numerical Recipes in C: The Art of Scientific Computing* (Second ed.); Cambridge University Press.
- Torres-Verdin, C., Victoria, M., Merletti, G. and Pendrel, J., 1999, Trace-based and geostatistical inversion of 3-D seismic data for thin-sand delineation: an application in San Jorge Basin, Argentina; *The Leading Edge*, 18(9), 1070–1077.
- Walker, C. and Ulrych, T. J., 1983, Autoregressive modelling of the acoustic impedance; *Geophysics*, 48, 1338–1350.
- Yilmaz, O., 2000, *Seismic data analysis: Processing, Inversion, and Interpretation of Seismic Data*; Society of Exploration Geophysicists.